THE MANTO-TYPE GOLD DEPOSITS OF ANDACOLLO (CHILE) REVISITED: A MODEL BASED ON FLUID INCLUSION AND GEOLOGIC EVIDENCE

ROBERTO OYARZUN, LORENA ORTEGA, JOSEFINA SIERRA, ROSARIO LUNAR,

Departamento de Cristalografía y Mineralogía, Facultad de C.C. Geológicas, Universidad Complutense, 28040 Madrid, Spain

AND JORGE OYARZUN

Departamento de Minas, Facultad de Ingeniería, Universidad de La Serena, Casilla 554, La Serena, Chile

Introduction

The Andacollo district is located in the Coquimbo region of Chile at 30°14′S to 71°06′W, some 55 km southeast of La Serena, at an elevation of 1,030 m, within a semiarid hilly landscape (Fig. 1). Mining activity initiated in pre-Colonial times when the Inca empire expanded southward (mid-fifteenth century). First the Incas, and later the Spaniards, exploited Andacollo for gold, mainly from auriferous gravels. By the end of the nineteenth century copper mining began. Early in this century a process involving in situ leaching was devised to recover copper (Concha et al., 1991). Renewed interest in gold mining in the district came in 1933 as a consequence of the world economic depression (Cuadra and Dunkerley, 1991). At present, mining activity in the district is concentrated on both copper and gold. A Tungsten-CMP joint venture is starting to mine copper from a porphyry deposit whereas Dayton Chile is extracting gold from manto-type deposits. Dayton has outlined some 29 million metric tons (Mt) of 1.2 grams per ton (g/t) Au (Bernstein, 1990), whereas other sources increase this figure to ~110 t of contained Au (Sillitoe, 1991).

The district (Fig. 1) comprises a variety of gold, copper, and mercury deposits. Central to the district is a porphyry copper of Cretaceous age (Andacollo porphyry). Manto-type epithermal gold deposits occur west of the porphyry, whereas gold veins occur to the northwest, west, and southeast. Mercury veins occur farther to the southeast (e.g., Dichosa; Fig. 1). The manto gold deposits, classified by Reyes (1991) as adularia-sericite type, are hosted by Lower Cretaceous volcanics of andesitic to dacitic composition. Both veins and manto-type deposits have been perceived as being genetically related to the main porphyry intrusion. The mantos have been considered as contact-metasomatic distal deposits (Sillitoe, 1983, 1991) or porphyry-related deposits (Llaumet, 1983; Müller, 1986; Camus, 1990; Reyes, 1991). Llaumet (1983) defined a series of mineralogic zones grading horizontally outward from the porphyry at the district scale. However, mineralogical and fluid inclusion studies, and a structural reappraisal of the district presented here indicate that an alternative geologic model can be proposed for the Andacollo adularia-sericite manto gold mineralization.

If the tilted, eroded structural blocks hosting the deposits are restored to their original horizontal prefaulting position, a vertical zoning is more evident. This stratigraphic-structural approach to the problem seems to fit the observed distribution of ore and alteration facies better, as described below. Moreover, fluid inclusion data from the mantos indicate a thermal gradient that does not support a porphyry-centered model based on the Andacollo intrusion, because the highest temperatures (around 365°C) are not found in the vicinity of the porphyry but some 4 km away. Furthermore, fluid evolution from moderate to high salinities during the cooling of the system suggests the presence of a hidden intrusion beneath the manto deposits, according to a model similar to the one described for Red Mountain, Arizona (Bodnar and Beane, 1980).

Geology

The mining district is mostly confined to a fault-bounded north-south depression (Andacollo basin; Fig. 2) partially filled with Tertiary gravels, some of them containing Au placer-type deposits. The geology of the district (Fig. 1) consists largely of the volcanic-volcaniclastic Quebrada Marquesa Formation of Barremian-Albian age (Aguirre and Egert, 1965; Rivano and Sepulveda, 1991). This formation can be ascribed to the so-called Ocoite Group (Aguirre et al., 1989), a 3- to 13-km-thick sequence extending for about 1,000 km along the Coastal Range of central-northern Chile. Most of the basic lavas belong to the high K calc-alkaline and shoshonite series (Levi et al., 1987), although a transition to the calc-alkaline series has been observed to the north. The Ocoite Group is affected by a nondeformational burial metamorphism ranging from the zeolite to greenschist facies (Åberg et al., 1984; Aguirre et al., 1989). This type of metamorphism is also known in Chile as the regional alteration.

The stratigraphy of the Quebrada Marquesa Formation at Andacollo is shown in Table 1. The Quebrada Marquesa Formation is intruded by a middle Cretaceous batholith varying in composition from diorite to tonalite (Reyes, 1991). Shallow intrusions related to the batholith include dikes, sills, and stocks, the latter well exemplified by the presence of the Andacollo porphyry (98 ± 2, 104 ± 3 Ma, whole-rock K/Ar ages, Reyes, 1991) of granodiorite-tonalite composition (Llaumet, 1983). Dikes and laccoliths are increasingly abundant to the east of the Andacollo fault (Pichilingo and Carbonica units), where according to Müller (1986) the highest intrusion levels were achieved (some 400 m above the Andacollo porphyry level).

Drilling carried out on the Andacollo porphyry copper deposit by ENAMI (Empresa Nacional de Minería, Chile) and Noranda in the late 1970s indicated 249 Mt grading 0.62 percent Cu, 0.25 g/t Au, and ~0.01 percent Mo. Andacollo is not to be regarded as a typical Chilean porphyry copper deposit (Llaumet, 1975), as it is older, does not lie within the main Cenozoic porphyry copper belt, and has relatively high Au grades.

The rocks were extensively block faulted and tilted by two

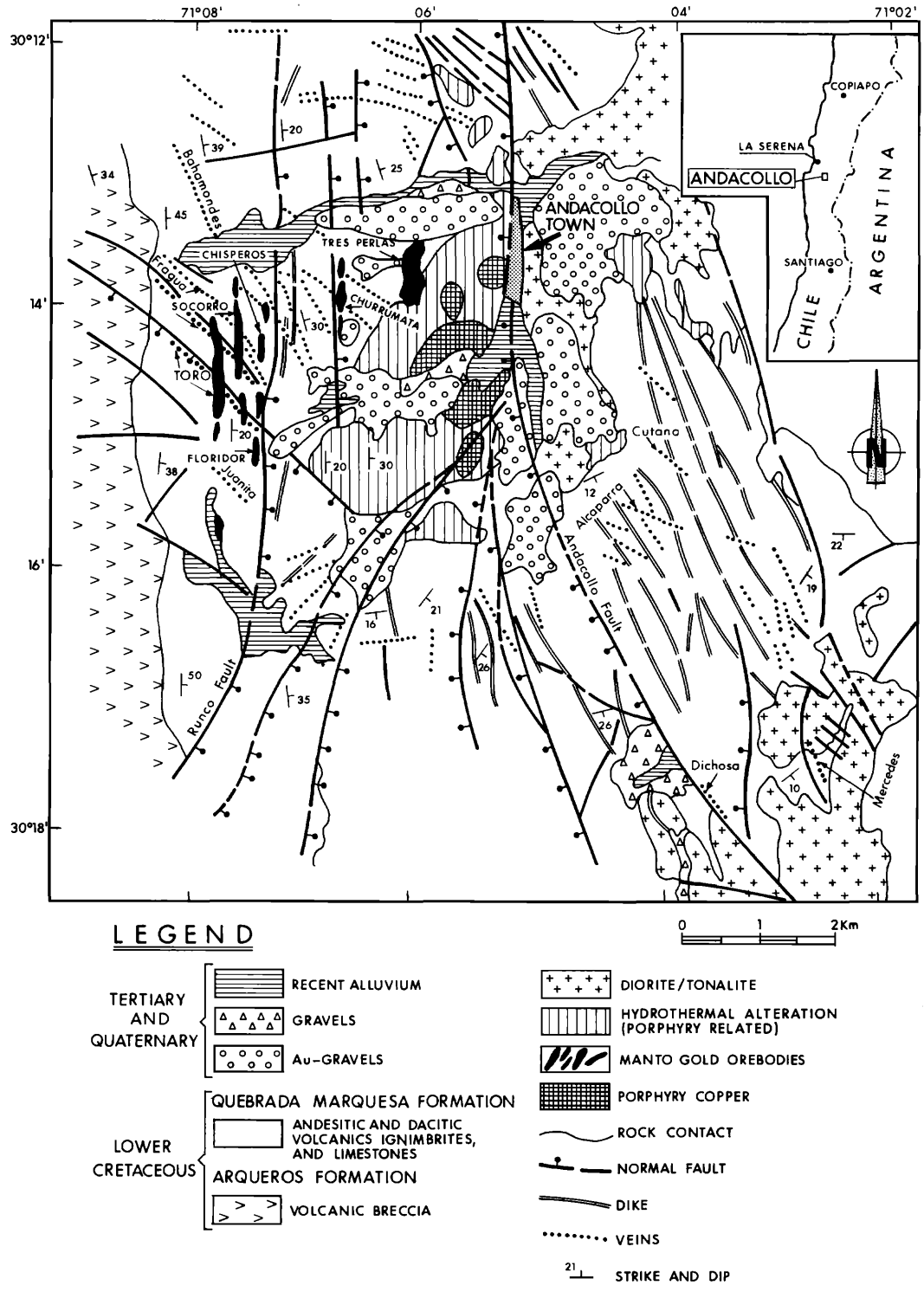

FIG. 1. Geologic map of the Andacollo district. Geology after Müller (1986) and Reyes (1991). Structural data reflect the general attitude in the given area. The alteration halo includes both the potassic (K feldspar, biotite) and quartz-sericite facies.

sets of extensional faults: northwest to east-west faults, dipping 50° to 90° to the southwest (premineral), and north-south (postmineral) faults of variable geometry (Figs. 1, 2; Reyes, 1991). The first set is of major importance as these faults allowed hydrothermal fluid circulation and deposition of minerals as veins and mantos. Later horizontal movements are revealed by slickensides developed in many veins of the district. The second set of faults is responsible for en echelon

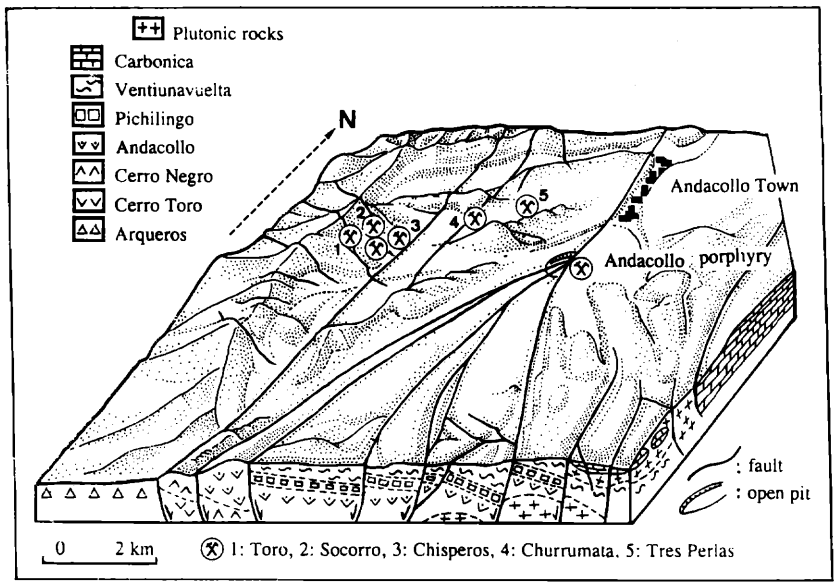

FIG. 2. Block diagram depicting the most outstanding morphological and structural features of the Andacollo district. Based on Müller (1986).

block faulting and tilting throughout the district and developed after intrusions and mineralizing processes took place. Among these, the Runco and Andacollo faults are the most important, the latter cutting across the Andacollo porphyry. Two kilometers to the south of the town of Andacollo, the Andacollo fault splits into several normal faults splays trending northwest to northeast (Figs. 1, 2). The present configuration of structural blocks in the district is largely due to the late fault system, which caused individual vertical displacements of up to 600 m. It is believed that faulting and associated block tilting initiated in the early Tertiary and may still be active (Müller, 1986). Stratigraphic-structural relationships for the whole Andacollo basin can be observed in Figure 2, whereas those for the mantos zone are depicted by Reyes (1991, fig. 6).

The variable orientations displayed by the structural blocks indicate a rotational movement of the extensional blocks (e.g., Twiss and Moores, 1992). The changes in dip shown by the beds (12°–45° to the east-southeast) belonging to well-defined structural units (bounded by major extensional faults) indicate an overall clockwise rotation of blocks, i.e., from east to west (Figs. 1, 2). This situation is particularly well defined within the eastern domain of the district. Further evidence is provided by the sedimentation of Tertiary gravels along a well-defined north-south trend to the east of the Andacollo fault, which indicates that tectonic subsidence must have been more important along this domain. Additional data supporting this interpretation is that the present extent of the alteration halo around the Andacollo porphyry abruptly disappears east of the Andacollo fault, indicating postmineralization faulting and block tilting. Some minor depocenters can be found also between the normal faults and within areas

TABLE 1. General Characteristics of the Andacollo Mantos and Selected Vein Deposits

Units	Rock types	Thickness (m)	Mantos	Veins	Ore type	Alteration	T(°C) (mode)[1]
Carbonica	Limestone, andesite, andesitic breccia	240		Dichosa, Mercedes	Hg-polymetallic	Opalization	<110[2]
Veintiuna Vuelta	Ignimbrite	350		Cutana, Alcaparra	Cu-Au-Pb	Propylitic	
Pichilingo	Andesite	200					
Andacollo	Andesite, volcanic flow breccia, dacite	800	Tres Perlas, Churrumata		Au-Cu-Zn-Pb	Propylitic, adularia, calcite, kaolinite	Tres Perlas: 295
Cerro Negro	Andesite	300		Bahamondes			
Cerro Toro	Andesite, dacite, volcanic flow breccia	680	Chisperos, Floridor, Socorro, Toro	Bahamondes, Fragua Juanita, Socorro, Toro	Au-Cu-Zn-Pb	Propylitic, adularia, calcite, kaolinite	Toro: 325, Bahamondes: 330, Chisperos: 310

Units of the Quebrada Marquesa formation are indicated on the left (in stratigraphic order, youngest at top); data from this work and from Müller (1986) and Reyes (1991)

[1] Homogenization temperatures for the ore stage (stage 1)

[2] Inferred from alteration type (after White and Hedenquist, 1990)

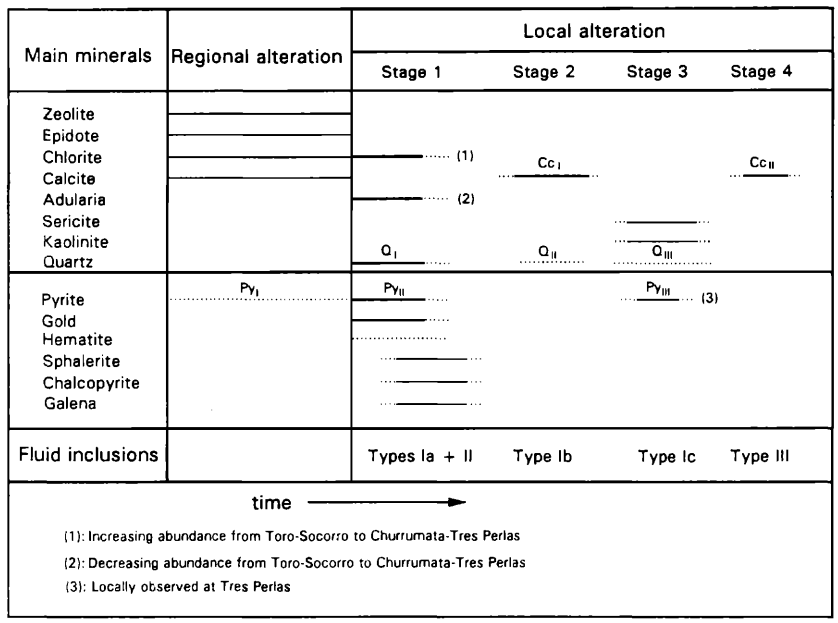

FIG. 3. Generalized paragenetic sequence (ore and alteration minerals) and associated fluid inclusion types for the manto-type deposits. Cc = calcite, Py = pyrite, Q = quartz.

bounded by the intersection of the north-south and northwest to east-west fault sets.

Andacollo Epithermal Gold Deposits

The Andacollo district includes a variety of vein-type deposits, but those strictly related to the gold manto-type mineralization occur west of the Andacollo porphyry (Figs. 1, 2). Veins are strongly controlled by the northwest-trending set of normal faults (Fig. 1). The manto-type mineralization is strata bound and largely confined to specific rock types (andesite breccias and dacites) and sites of strong fracturing. Müller (1986) and Reyes (1991) distinguished three zones of mantos from west to east: Toro-Socorro (including manto Chisperos), Churrumata, and Tres Perlas (Fig. 1; Table 1). Both lateral and vertical continuity of the mantos is strongly controlled by rock type, the northwest set of extensional faults and intensity of fracturing. The northwest faults acted as channels for fluid circulation, ultimately leading to both vein- (vertical circulation) and manto-type (horizontal circulation) mineralization. In the andesites and andesite flow breccias the mineralization extends not only horizontally but vertically in response to rock fracturing and porosity (e.g., Toro, Socorro). In the dacite beds the mineralization is mostly confined to the top vesicular parts of flows (e.g., Churrumata, Tres Perlas), extending vertically only where fracturing allowed the solutions to pass through (Reyes, 1991). Hydraulic brecciation has been observed at Andacollo, particularly in the Socorro manto (Müller, 1986).

The mantos are characterized by a relatively simple paragenesis (Fig. 3), including two generations of pyrite. The earliest one (pyrite I; premineralization) is barren and the second (pyrite II) is gold bearing. The ore stage also includes sphalerite with exsolutions of chalcopyrite, minor chalcopyrite, and galena. Pyrite I occurs either as irregularly shaped isolated grains or as cores within larger pyrite II crystals. Pyrite II is easily recognizable as it occurs as large, almost perfect cubes of up to 10 mm. A late generation of pyrite (III) quartz veinlets with sericite-kaolinite halos is recognized in the Tres Perlas deposit. Ore grades range from 2 to 8 g/t Au (Reyes, 1991). Main gangue minerals are quartz and calcite which deposited along four stages (Fig. 3). Stage 1 is characterized by idiomorphic to subidiomorphic quartz crystals (Q_I), which accompanied the main ore deposition. Stage 2 resulted in the precipitation of coarse-grained calcite (Cc_I). In addition, recrystallization of early quartz took place during stages 2 and 3 (with precipitation of Q_{II} and Q_{III}, respectively), as shown by secondary fluid inclusions in Q_I. Q_{III} is also observed as fine-grained quartz in Churrumata and Tres Perlas, locally replacing previous calcite (Cc_I). Finally, stage 4 corresponds to microcrystalline calcite (Cc_{II}) which, in the Toro deposit, also recrystallized calcite I, as indicated by fluid inclusion evidence. Other gangue minerals include chlorite and hematite.

The veins are mineralogically similar to the mantos, even though the gangue is mostly composed of quartz, sometimes of the amethystine variety. Gold grades average in the range of 5 to 6 g/t Au, even though the oxidation zone may locally yield values as high as 300 g/t Au (Reyes, 1991). Examples of these veins are Socorro, Toro, and Bahamondes, which are hosted by the volcanics of the Cerro Toro, Cerro Negro, and Andacollo units (Fig. 1; Table 1). Gold vein-type mineralization persists to the southeastern sector of the district. There the veins are hosted by the Pichilingo and Veintiuna Vuelta volcanics. The latter marks the transition toward mercury veins hosted by limestones belonging to the Carbonica unit (Müller, 1986). These veins are characterized by the presence of Hg tetrahedrite (schwazite), pyrite, chalcopyrite, bornite, and galena. Gold contents in these veins are negligible. A very late generation of veins within the Andacollo district are barite rich and are confined to the Churrumata area. They

occur along the late north-south faults and with a single exception crosscut the earlier northwest veins.

Hydrothermal Alteration

Manto-type deposits and related veins

Based on textural relationships the following alteration sequence can be established for the manto-type deposits (Fig. 3): propylitic (regional alteration, preore: chlorite, calcite, epidote, zeolite) → adularization (accompanied by quartz veining) + chloritization + hematite → carbonatization I (calcite veining) → sericite + kaolinite → carbonatization II. This sequence correlates with the stages of mineral deposition described above (Fig. 3). Sulfide gold deposition is part of the adularia quartz stage. Pyrite I is very early and may be related to the regional propylitization. Adularia represents the earliest local alteration phase and is related to a very strong K metasomatism affecting the volcanics. Mean values of K_2O range from 5.28 percent in the Andacollo unit to 8.06 to 9.75 percent in the Cerro Toro unit (Müller et al., 1988). Kaiser (1942) found values of 3 percent K_2O in the unaltered andesites and 8 percent K_2O (avg) in those with strong alkalinization (Socorro Manto; Cerro Toro unit). Data obtained by Müller et al. (1988; range in the Cerro Toro unit = 4–14% K_2O; n = 25) confirm this further.

The relative proportions of potassium, thorium, and uranium are useful in differentiating lithologies and in discriminating between rocks naturally rich in potassium and potassium metasomatic alteration zones (Irvine and Smith, 1990). Furthermore, the ^{40}K component of the total gamma radiation detected in radiometric surveys is a useful indicator of the intensity of the adularia alteration and hence of the gold-rich portions of the deposit (Allis, 1990; Irvine and Smith, 1990). A surface gamma ray survey in the Andacollo district with a portable GIS-5 Scintrex instrument showed that the highest values (>4,000 c/s) concentrate within the area where the mantos are located, particularly within the Toro-Socorro area (Fig. 4). Since two-thirds of the total counts measured in the survey correspond to the ^{40}K radiation, we can assume that the values reflect the extension and intensity of the potassic alteration zone. This is in agreement with what Reyes (1991) defined as a potassic gradient in the Mantos zone, with adularia increasing from Tres Perlas to Socorro, i.e., from east to west regardless of the rock type (e.g., andesite flow breccias with and without adularia at Socorro and Tres Perlas, respectively). Conversely, at Tres Perlas and Churrumata the main alteration stage (gold deposition) is mostly characterized by chlorite, which decreases toward the Toro-Socorro zone.

Adularia occurs as small idiomorphic crystals in quartz, some of them displaying the rhombic cross section. Calcite (I) occurs as large crystals within veins and veinlets. The sericite-kaolinite alteration was strong and resulted in almost total replacement of feldspar and early adularia by this assemblage. Calcite (II), very fine grained and dispersed within the rock matrix, represents a late stage of intense carbonate deposition. Both the sericite-kaolinite and carbonatization give the andesitic rocks a characteristic pale pinkish color (e.g., Cerro Toro andesites).

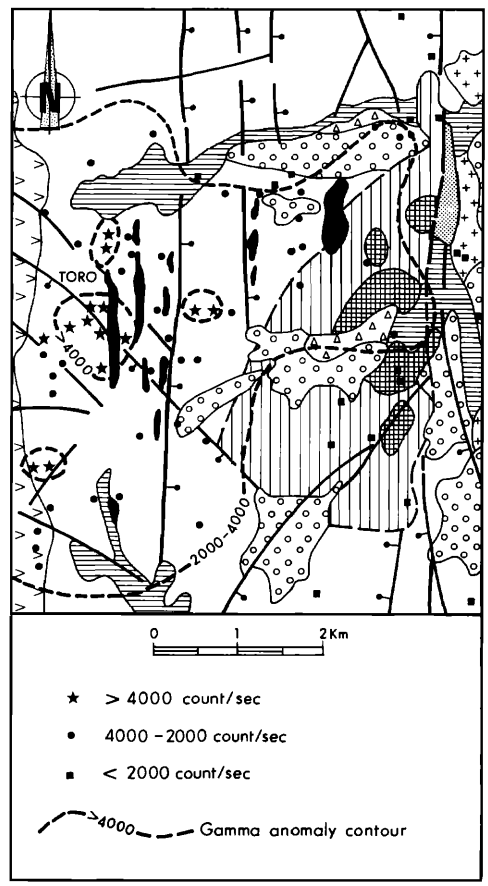

FIG. 4. Gamma ray anomalies (2,000–4,000 and >4,000 c/s) in the western sector of the Andacollo district. Instrument: Scintrex GIS-5.

Other alteration types within the district

The Andacollo porphyry (Fig. 1) displays several alteration types. First, potassic alteration, as defined by the presence of K feldspar and biotite with pyrite-chalcopyrite-molybdenite mineralization: this alteration can be observed in the surface, although it is better developed in depth; it grades outward into a propylitic facies defined by chlorite, calcite, and epidote. Second, quartz-sericite alteration locally overprints the former asssemblages. Third, veins other than those related to the manto-type gold deposits typically display propylitic alteration. An exception is provided by the mercury veins in the eastermost part of the district. There the limestone country rocks (Carbonica unit) are strongly silicified by opaline silica, forming up to 10-m-wide halos flanking the veins. This alteration type can be interpreted as resulting from silica saturation at temperatures below 110°C (White and Hedenquist, 1990).

The mercury deposits have negligible gold values and may be marking a gold-depleated zone of the district. In fact, the southeasternmost gold veins are restricted to the ignimbrites of the Veintiuna Vuelta unit (lying inmediately beneath the Carbonica unit; Table 1). The variable character of these veins is demonstrated by the mineralogical change observed along the passage from the rhyolites (Veintiuna Vuelta unit) to the limestones (Carbonica unit). The change is well de-

picted by a galena-sphalerite-chalcopyrite-(tetrahedrite) vein with contents of up to 100 g/t Au in the Veintiuna Vuelta unit. When entering the limestone rocks, the vein loses the gold and cinnabar appears (Müller, 1986). Although some of the Hg veins are hosted by the Veintiuna Vuelta unit, the higher mercury contents are always restricted to those veins hosted by the limestones of the Carbonica unit; this may be the result of differential chemical reactivity of the country rocks.

Age of Mineralization and Stratigraphic-Structural Relationships

At a regional scale the Early to middle Cretaceous plutonism took place along a north-south belt during the time span 130 to 87 Ma (Zentilli, 1974; Sillitoe, 1981; Berg and Breitkreuz, 1983; Boric, 1985) and can be regarded as emplaced during an early stage of the Cretaceous volcano-plutonic arc development (Reyes, 1991). The plutonic activity was fairly continuous and overlapped the volcanism, although it reached a maximum during the middle Cretaceous (Åberg et al., 1984).

Based on the information provided by K-Ar dates for the Andacollo district (Reyes, 1991), the ages of the altered gold-bearing rock (91 ± 6 Ma) and the porphyry (104 ± 3, 98 ± 2 Ma) can be regarded as similar. However, the discrepancy of about 7 to 13 m.y. may be significant in defining the gold mineralization as relatively younger than the porphyry copper. The Barremian-Albian age of the host rocks indicates that at least the uppermost units of the Quebrada Marquesa Formation (e.g., Carbonica) were still being deposited when plutonism and mineralizing processes were taking place at Andacollo and were probably horizontal. From a geologic point of view this is of major relevance since the stratigraphic positions occupied by the different manto deposits are in this case reflecting the depth at which they formed. As discussed earlier, block faulting-tilting is postmineral (Tertiary age). This means that the exposed manto deposits represent the posttilting, posterosion mineralized remnants of larger bodies occurring within favorable stratigraphic levels (which may contain other, yet to be found, equivalent deposits). An inspection of the local stratigraphic column reveals that the Toro-Socorro-Chisperos and Churrumata-Tres Perlas manto zones are located within the Toro and Andacollo units, respectively, i.e., they are stratigraphically beneath some 2,200 and 1,200 m of volcanic-volcanoclastic-sedimentary rocks, respectively. These figures can therefore be used as a geologic estimation of the minimum paleodepth of formation of the manto deposits.

Fluid Inclusions

Typology and occurrence of inclusions

Fluid inclusion studies were carried out in 16 samples of quartz and calcite from Toro, Chisperos, Churrumata, and Tres Perlas mantos and in two samples of quartz from the Bahamondes vein. Regarding the Andacollo porphyry, the state of the mining works at the time of sampling did not allow samples to be obtained suitable for fluid inclusion studies. Microthermometric measurements were performed using a Chaixmeca cooling and heating stage on a Nikon Labophot microscope. The fluid inclusions are largely aqueous and contain dissolved salts, in some cases resulting in the presence of daughter halite crystals. The absence of major volatiles other than H_2O was confirmed by Raman analyses. Classification of fluid inclusions was based on microthermometric behavior and phase relations observable at room temperature. Three different types of fluid inclusions have been distinguished: type I, liquid rich; type II, vapor rich; and type III, halite bearing. The latter also include inclusions with salinities higher than 23 wt NaCl equiv but lacking daughter minerals due to significant amounts of salts other than NaCl. These inclusion types are similar to those described in porphyry copper deposits (Roedder, 1971; Nash, 1976).

Type I inclusions are two phase and liquid rich inclusions with a vapor bubble generally occupying between 0.1 and 0.4 of the total volume of the inclusion. They are very abundant and show regular morphologies and a size between 3 and 40 μm. Three populations of inclusions can be distinguished, based upon their degree of filling (vapor volume($V_{(v)}$)/total volume($V_{(t)}$)) and their mode of occurrence: Ia ($V_{(v)}/V_{(t)}$ = 0.3–0.4); Ib (0.15–0.25), and Ic ($\leq$0.1). They are found in all the mantos and in the Bahamondes vein. Type Ia inclusions are only observed in the early quartz (Q_I, stage 1) and occur as isolated inclusions, in groups, or in alignments which parallel quartz growth faces, thus indicating a primary origin. They often share the same rows with monophase inclusions (type II) and occur in the same areas as planar arrays of type II inclusions, suggesting the existence of a heterogeneous fluid during trapping (Roedder, 1984). These features were observed in the Toro, Chisperos, and Tres Perlas mantos and in the Bahamondes vein, whereas quartz from the Churrumata manto exhibited very scarce fluid inclusions. Further textural evidence to support this hypothesis is locally found in the Chisperos manto, where alignments of coexisting two-phase and monophase inclusions show type Ia inclusions with a highly variable degree of filling between 0.3 and 0.8. These inclusions could represent the mechanical trapping of both liquid and vapor phases resulting from boiling. Microthemometric data indicate that type Ia inclusions show a moderate salinity, with most inclusions in the range of 5 to 10 wt percent NaCl equiv for all the deposits (Figs. 5 and 6). Only a few inclusions from the Bahamondes vein and the Tres Perlas manto exceed these figures and show salinity values up to 20 wt percent NaCl equiv. Homogenization temperatures range between 275° and 365°C (into liquid), although inclusions from the Toro and Bahamondes mantos generally homogenized at higher temperatures than those from the other deposits (Figs. 5 and 6).

Types Ib and Ic occur as secondary inclusions in separate fractures crosscutting the quartz (Q_I), and they correspond to stages 2 and 3, respectively. Type Ib inclusions ($V_{(v)}/V_{(t)}$ = 0.2) are also observed as primary inclusions showing ramdom three-dimensional distribution in calcite I (stage 2) in the different deposits, postdating the main mineralizing event. Salinity values for type Ib and Ic inclusions generally fall between 3 and 10 wt percent NaCl equiv; however, some scattered higher values are observed in the Tres Perlas manto. Temperatures of homogenization range from 210° to 290°C for type Ib inclusions, with similar values in all the mantos (Figs. 5 and 6). Some monophase inclusions occur among

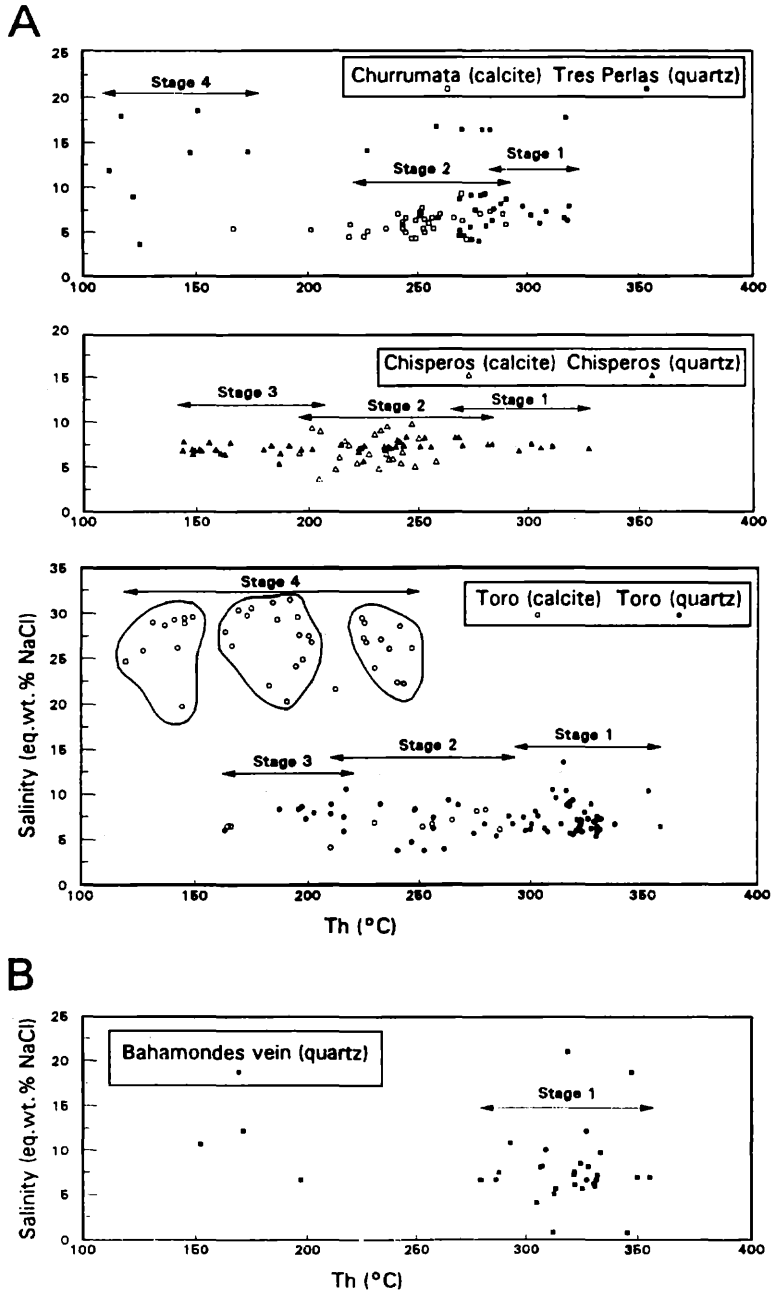

FIG. 5. Salinity vs. homogenization temperature diagram for fluid inclusions from mantos (A) and veins (B).

type Ib inclusions at Tres Perlas. In most of the inclusions, melting of ice was observed between −2.5° and −6°C, and occasionally, a vapor bubble nucleated on cooling, indicating a metastable behavior of otherwise two-phase inclusions. The Bahamondes vein did not show type Ib inclusions suitable for microthermometric studies. Type Ic inclusions were also difficult to study due to their small size. This explains the scarcity of measurements for most of the deposits, except for Chisperos and Toro, which show homogenization temperatures in the range 135° to 215°C and 165° to 220°C, respectively.

Much less abundant than type I inclusions, type II inclusions are monophase inclusions at room temperature which show rounded regular shapes and range in size from 5 to 15 μm. They occur in quartz (Q_I) from all the mantos and the Bahamondes vein within planar arrays containing multiple monophase inclusions and with type Ia inclusions in the same alignments. They are primary and were trapped contemporaneously with two-phase type Ia inclusions during stage 1. No phase transitions were observed in type II inclusions during the microthermometric runs, and the Raman studies show no volatiles.

Type III inclusions are high-salinity, two-phase liquid-rich and three-phase halite-bearing ones. The latter contain a sin-

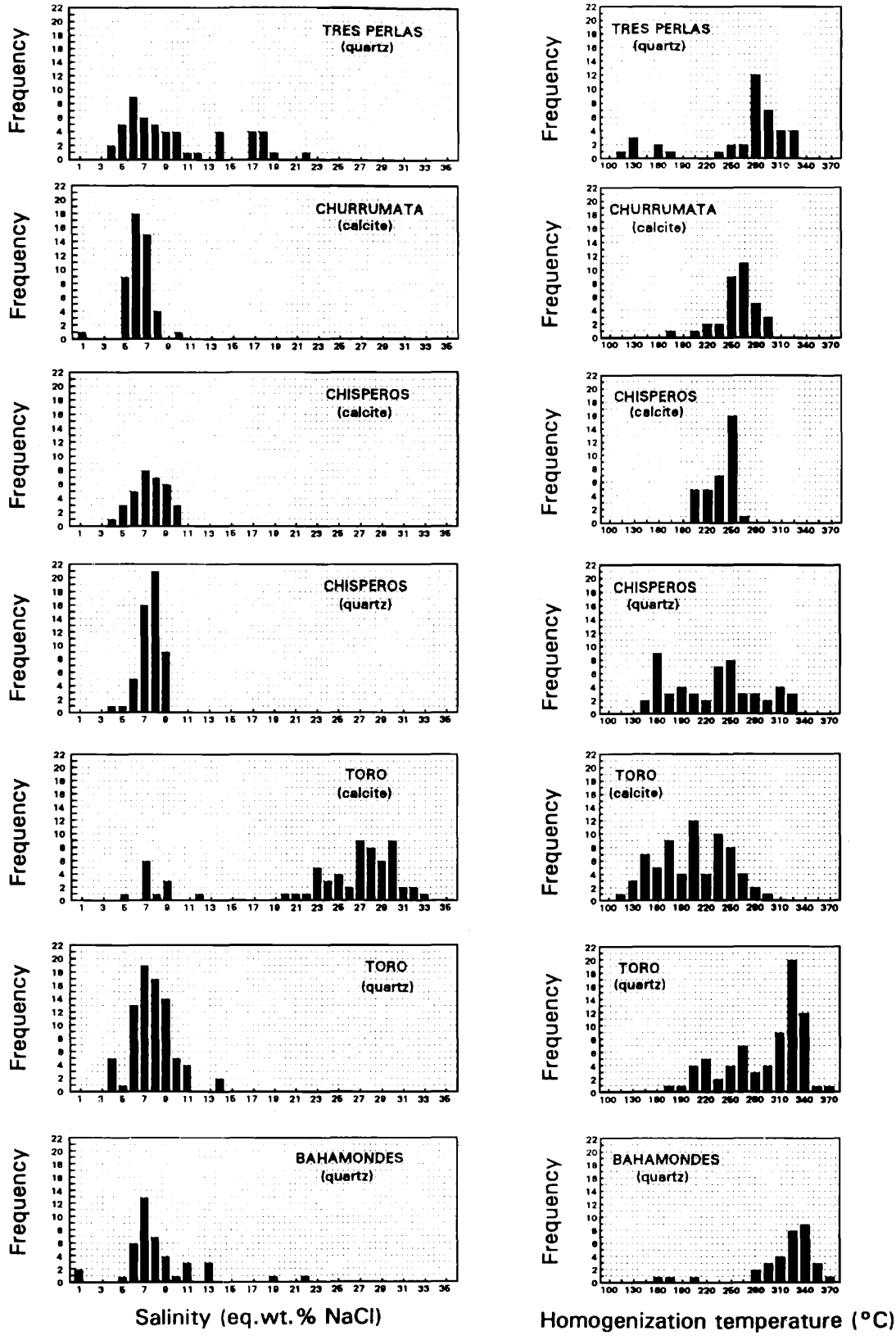

FIG. 6. Histograms of salinity (wt % NaCl equiv) and homogenization temperatures (°C) for the Toro, Chisperos, Churrumata, and Tres Perlas mantos and the Bahamondes vein.

gle daughter crystal which dissolves on heating. They show a degree of filling between 0.1 and 0.35 and range in size from 4 to 15 μm. These inclusions have only been found in calcite I from the Toro manto and show either calcite-negative crystal shapes or irregular morphologies. Type III inclusions are very abundant and occur in groups and in planar arrays following calcite cleavage directions. They are considered to be secondary in origin, postdating type Ib inclusions which appear as relics in the same calcite.

Salinities of type III inclusions containing halite at room temperature were obtained from the temperature of dissolution of halite and data for NaCl solubility given by Potter et al. (1977). For those inclusions undersaturated with respect to NaCl, salinities were estimated from the melting temperature of ice. Overall, salinity values range between 20 and 33 wt percent NaCl equiv, with most values between 26 and 30 wt percent NaCl equiv. Salt contents for three-phase halite-bearing and two-phase inclusions form a continuous range (Fig. 6), thus indicating that these two types of inclusions represent a single fluid with a composition lying across the NaCl saturation curve. These inclusions show first ice-melting temperatures around −56°C, indicating the presence of salts other than NaCl. This is confirmed by qualitative scanning electron microscope(SEM-EDS) analyses on frozen fluid inclusions, showing that the dissolved salts are mostly NaCl and $CaCl_2$, with minor amounts of KCl. The presence of $CaCl_2$ in significant amounts can explain the occurrence of a number of inclusions with the melting of ice down to −34°C (32 wt % NaCl equiv) in the absence of halite daughter crystals. Since salinity is expressed as wt percent NaCl equiv, it reflects not only the NaCl content but an estimation of the total amount of dissolved salts. Furthermore, NaCl saturation in such a fluid will not occur at ~26 wt percent NaCl as it would in the pure NaCl-H_2O system (Roedder, 1984). Total homogenization values of liquid in the two-phase inclusions are between 110° and 250°C (approx 60% of the total population), by either vapor bubble or halite disappearance in the halite-bearing inclusions. The latter inclusions must have been trapped in the vapor-absent field of the NaCl-H_2O system (Bodnar, 1994; Cline and Bodnar, 1994).

Occasionally, monophase and two-phase (halite + fluid) inclusions have also been observed in calcite from the Toro manto, associated with type III inclusions. They may have resulted either from leakage or from a failure to nucleate a vapor bubble in some type III inclusions.

Fluid circulation history

The liquid-rich, moderate-salinity type I inclusions are by far the most common ones in the Andacollo gold district. In this fluid inclusion type, the different gold deposits share a similar pattern of fluid evolution with a decreasing trend of homogenization temperatures from 365° to 100°C. This range can be divided into three major groups (Fig. 5), corresponding to the main local alteration and mineral deposition stages in the deposits. The first group (adularia + hematite + quartz + gold-bearing pyrite) shows homogenization temperatures with maximum frequency at 325°C for Toro, 310°C for Chisperos, and 295°C for Tres Perlas. The Bahamondes vein, sampled close to the Toro manto, also shows a main population of high temperature with most values around 330°C. This distribution reveals some differences between the deposits located in the lowest unit of the volcanic stratigraphic sequence (Toro and Chisperos) and those located in the stratigraphically higher Andacollo unit (Churrumata and Tres Perlas). Toro fluid inclusions show the highest temperatures of the area (up to 365°C, Figs. 5 and 6) whereas these values decrease toward the stratigraphycally more shallow mantos (up to 320°C in Tres Perlas). The second group (calcite + quartz) exhibits similar ranges of homogenization temperatures for all the mantos, although maximum frequencies vary slightly between 250° and 275°C from one deposit to another. The third group (kaolinite + sericite + quartz) is not well depicted by fluid inclusions in Churrumata, Tres Perlas, and Bahamondes. Most homogenization temperatures are around 220°C in Toro and 165°C in Chisperos.

The Toro manto exhibits a feature which distinguishes it from the other deposits: the presence of a high-salinity fluid, represented by type III inclusions. These inclusions are secondary in coarse-grained calcite (CcI)and only occur in the Toro manto. They correspond to the late intense carbonatization (stage 4) observed in the area. In this hypersaline population, three different groups can be again distinguished (Fig. 5), suggesting the existence of different pulses of fluid circulation with median homogenization temperatures of around 235°, 180°, and 140°C, respectively. Halite-bearing inclusions occur mostly in the two lower temperature groups, and in those inclusions, homogenization by halite dissolution is lower in salinity. This sequence of fluid inclusion trapping is to be expected from a brine following a cooling path (Bodnar, 1994). Homogenization temperatures of this high-salinity fluid are shifted to lower values compared to those of the type I low-salinity inclusions, and although a significant overlap does exit, the high-salinity fluid postdates the low-salinity one.

An important characteristic of the hydrothermal system is the evidence of boiling during the early stage of mineral deposition. Such a process is recognized by the temporal coexistence of vapor-rich inclusions (type II) with liquid-rich two-phase inclusions (type Ia) which represent the vapor and the liquid fractions, respectively, of the boiling fluid. Because inclusions trapped along the boiling curve require no pressure correction, homogenization temperatures are the same as trapping temperatures (Ramboz et al., 1982). Therefore, Bahamondes and Toro higher temperatures around 365°C, Chisperos at 325°C, and Tres Perlas at 320°C are the upper limit of the actual temperatures of fluid circulation during stage 1 at the different deposits. Boiling is also supported by other evidence, such as the existence of hydraulic brecciation at the Socorro manto (in the same stratigraphic level as the Toro manto) and the occurrence of mineralogical indicators (Browne and Ellis, 1970; Browne, 1978; Henley, 1985; Hedenquist, 1990; Dong and Morrison, 1995) as adularia, hematite, and calcite.

Further considerations on the process of boiling can be made based on geologic data. As established previously, the volcanic sequence was not tilted at the time of mineralization and therefore the paleodepth of mantos sites at formation time can be estimated from the stratigraphic column: 2,200 m for Toro, 2,000 m for Chisperos, 1,400 m for Churrumata, and 1,000 m for Tres Perlas. In this environment the pressure

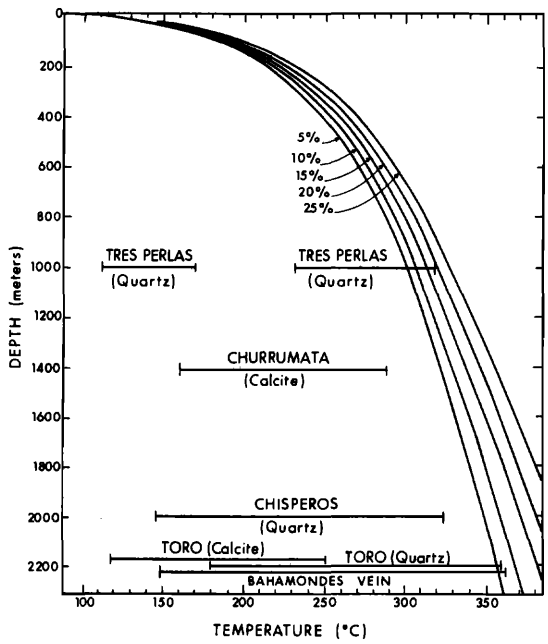

FIG. 7. Boiling point curves for the H_2O-NaCl system (Haas, 1971). Range of homogenization temperatures for the different mantos and the Bahamondes vein have been plotted as straight lines. Depths of deposits have been assumed according to the model here proposed.

regime is most likely to have been hydrostatic because this type of pressure can extend up to 3 km beneath the surface in geothermal fields (White and Hedenquist, 1990). Under these circumstances, the inspection of the fluid inclusion data with temperature vs. depth of boiling curves (Haas, 1971) can be useful in confirming the existence of boiling in the different manto sites. Homogenization temperatures of fluid inclusions from the mantos and data of Haas (1971) have been plotted in Figure 7. Results indicate that some boiling may have occurred at the very early stages of fluid circulation (type Ia fluid inclusions with higher homogenization temperatures) at the Toro and Tres Perlas mantos. However, Chisperos homogenization temperatures do not intersect the boiling curves even though unambiguous fluid inclusion evidence of boiling has been observed in this manto. This may be due to the presence of undetected CO_2 in the system since small contents of CO_2 would shift the boiling curves toward lower temperatures (Sutton and McNabb, 1977; Henley, 1985). This volatile was not detected either by Raman spectroscopy or by microthermometry, although the important amounts of calcite in the district indicate that it is present in the fluids. Boiling also may have occurred at given sectors of the veins, as observed in the Bahamondes vein (sampled at the Toro manto level) at a stratigraphic depth of over 2,200 m (Fig. 7). Therefore, boiling fluids characterized the adularia alteration stage through the entire volcanic pile and were also responsible for ore mineral deposition, with the precipitation of gold-bearing pyrite. During the carbonatization (I) and sericitization stages, the fluids followed a simple cooling path (Fig. 5).

In the high-salinity type III inclusions trapped in the later stage of fluid circulation at the Toro manto, the possibility of boiling can be discarded according to Figure 7 and petrographic observations. Cline and Bodnar (1991) have shown that high-salinity fluids can be generated even in absence of boiling by calc-alkaline magmas and this is most likely to be the case of the brine trapped as type III fluid inclusions at the Toro manto. Mixing of this brine with cool and diluted meteoric waters at higher stratigraphic levels could have yielded a fluid of intermediate salinity as observed at Tres Perlas (Fig. 5, stage 4).

Discussion and Proposal of a Model

The Andacollo district has been interpreted previously as a hydrothermal system involving the formation of vein and manto-type deposits in response to the emplacement of a central porphyry Cu system (Andacollo porphyry; Reyes, 1991), which we will now call the "horizontal zoning model." However, a series of facts raise some doubts as to the validity of such a model.

Fluid circulation within a porphyry environment is expected to be broadly vertical, affecting mainly the preore cover above the heat source (Bodnar and Beane, 1980). For any model of fluid circulation or alteration pattern (e.g., Lowell and Guilbert, 1970; Gustafson and Hunt, 1975; Beane and Titley, 1981), the lateral influence of the intrusion decreases as depth increases within an overall balloon-shaped geometry. The isotherms are closely spaced on the sides of the intrusion; however, above the porphyry they are laterally and vertically extended by the upwelling convecting waters heated by the intrusion (Beane and Bodnar, 1995). Based on age and structural relationships, we have shown that the Quebrada Marquesa volcanics were probably in a horizontal position during intrusive activity and mineralization. Thus, the western mantos (Toro-Socorro-Chisperos; Toro unit) formed within a deeper environment than the eastern ones (Churrumata-Tres Perlas; Andacollo unit). Consider the Toro manto, which displays a series of characteristics that are of major importance to the understanding of the hydrothermal system: it is emplaced within the lowest stratigraphic unit, it records the highest temperatures of fluid circulation (T_h = up to 365°C), and it shows evidence of a late, high-salinity fluid. If the Andacollo porphyry is considered to be the center of the hydrothermal system (horizontal zoning model), Toro becomes the farthest manto-type gold mineralization but records the highest temperatures of fluid circulation. Another issue is the fluid evolution within the system. Contrary to classic examples of epithermal mineralizations (e.g., Creede; Hayba et al., 1985), the Toro manto shows evidence of a late, high-salinity fluid. Such a fluid is most likely to be of magmatic origin, similar to those fluids observed in porphyry copper deposits (e.g., Bodnar and Beane, 1980; Cline and Bodnar, 1991). Within a horizontal zoning model one would expect that this fluid was exsolved from the Andacollo porphyry. If that were the case, why is there no evidence of such a fluid in the nearer manto outcrops?

Let us consider a different approach to the problem: a vertical zoning model. As discussed by Bodnar and Beane (1980) for Red Mountain (Arizona), the existence of a late high-salinity fluid postdating a fluid of moderate salinity could be indicative of the presence of a hidden pluton beneath the altered volcanic cover. Under these conditions the first fluids

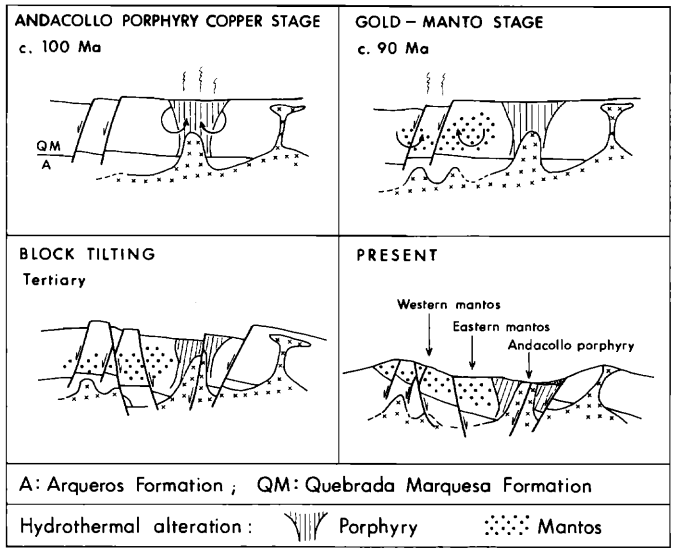

FIG. 8. Schematic model (looking north) for the development of the Andacollo hydrothermal system in space and time.

to flow within the lithocap would be those derived from the wall-rock environment, which would be followed by fluids originating from the underlying intrusion. Furthermore, lateral distal fluid circulation around a porphyry would be characterized by low salinity and would not evolve toward high-salinity types (Beane and Titley, 1981). Thus, considering the fluid types and their evolution (type I → type III at Toro), it can be proposed that the hydrothermal system which led to the manto-type gold mineralization was not driven by the Andacollo porphyry (on a lateral position) but by another intrusion, hidden beneath the mantos (vertical model). Another geologic feature supporting this interpretation is given by the alteration pattern along the mantos. Adularia is an important phase within the western mantos only. In porphyry environments adularia-sericite gold deposits form at shallow and distal sites (Sillitoe, 1989). Since the western mantos represent the lowest stratigraphic level, the intrusion in this case should be relatively deep and probably hosted by the Arqueros Formation (underlying the Quebrada Marquesa Formation). Geologic evidence supporting this idea is given by the increasing depth of intrusion levels from east to west in the Andacollo district.

Within this context we propose the existence of a different, gold-rich hydrothermal system later in time from the one that led to the Andacollo porphyry copper mineralization. Finally, we stress the importance of the pretilting structural approach to the problem. The present outcrop configuration in the area is misleading in many aspects and gives, at first glance, the impression of a classic case of horizontal zoning around a porphyry copper deposit. However, as shown and discussed in this work, the structural frame of the district when mineralizing processes were taking place was significantly different from the one observed at present, i.e., a rather horizontal sequence of volcanic and volcanosedimentary rocks being intruded at depth by plutonic rocks. We can envisage under these conditions a complex hydrothermal history involving at least two main episodes (Fig. 8): an early porphyry copper one, and a late manto and vein episode related to gold mineralization. The Hg veins cutting across the Carbonica unit might represent the uppermost part of the epithermal system. The original spatial distribution of the mineralized bodies was disrupted by later extensional faulting and block-tilting rotation in early Tertiary time, leading to the present structural configuration of the district (Fig. 8).

Acknowledgments

We thank Dayton Chile for facilities provided for visiting the Andacollo gold deposits in 1993 and 1994. P. Murphy and S. Roberts (Department of Geology, University of Southampton, UK) are acknowledged for assisting with the Raman analyses and J. García Veigas (University of Barcelona, Spain) for the SEM-EDS analyses in frozen inclusions. The original manuscript benefited from suggestions provided by two *Economic Geology* reviewers. We also thank R.J. Bodnar for several useful comments made to the authors during the 13th ECROFI Conference (Sitges, Spain).

June 16, 1995; October 25, 1996

REFERENCES

Åberg, G., Aguirre, L., Levi, B., and Nyström, J.O., 1984, Spreading-subsidence and generation of ensialic marginal basins: An example from the early Cretaceous of central Chile: Geological Society [London] Special Publication 16, p. 185–193.

Aguirre, L., and Egert, E., 1965, Cuadrángulo Quebrada Marquesa, Provincia de Coquimbo: Instituto de Investigaciones Geológicas (Chile), 92 p.

Aguirre, L., Levi, B., and Nyström, J.O., 1989, The link between metamorphism, volcanism, and geotectonic setting during the evolution of the Andes: Geological Society [London] Special Publication 43, p. 223–232.

Allis, R.G., 1990, Geophysical anomalies over epithermal systems: Association of Exploration Geochemists Special Publication 16b, p. 339–374.

Beane, R.E., and Bodnar, R.J., 1995, Hydrothermal fluids and hydrothermal alteration in porphyry copper deposits: Arizona Geological Society Digest, no. 20, p. 83–93.

Beane, R.E., and Titley, S.R., 1981, Porphyry copper mineralization. Part II. Hydrothermal alteration and mineralization: ECONOMIC GEOLOGY 75TH ANNIVERSARY VOLUME, p. 235–269.

Berg, K., and Breitkreuz, C., 1983, Mesozoiche Plutone in der Nord Chilenischem Küstecnkordillere: Petrogenese, Geochronologies, Geochemie und Geodynamik mantel bertonter Magmatite: Geotektonic Forschung, v. 66, p. 1–107.

Bernstein, M., 1990, The geology of copper and gold ore deposits in Chile: Mining Magazine, September 1990, p. 155–168.

Bodnar, R.J., 1994, Synthetic fluid inclusions: XII. The system H_2O-NaCl. Experimental determination of the halite liquidus and isochores for a 40 wt% NaCl solution: Geochimica et Cosmochimica Acta, v. 58, p. 1053–1063.

Bodnar, R.J., and Beane, R.E., 1980, Temporal and spatial variations in hydrothermal fluid characteristics during vein filling in preore cover overlying deeply buried porphyry copper-type mineralization at Red Mountain, Arizona: ECONOMIC GEOLOGY, v. 75, p. 876–893.

Boric, R., 1985, Geología y yacimientos metalicos del distrito Talcuna, IV Región de Coquimbo: Revista Geológica de Chile, v. 25–26, p. 57–75.

Browne, P.R.L., 1978, Hydrothermal alteration in active geothermal fields: Annual Review of Earth and Planetary Science Letters, v. 6, p. 229–250.

Browne, P.R.L., and Ellis, A.J., 1970, The Ohaki-Broadlands hydrothermal area, New Zealand: Mineralogy and related geochemistry: American Journal of Science, v. 269, p. 97–131.

Camus, F., 1990, The geology of hydrothermal gold deposits in Chile: Association of Exploration Geochemists Special Publication 16b, p. 197–232.

Cline, J.S., and Bodnar, R.J., 1991, Can economic porphyry copper mineralization be generated by a typical calc-alkaline melt?: Journal of Geophysical Research, v.96, p. 8113–8126.

—— 1994, Direct evolution of brine from a crystallizing silicic melt at the Questa, New Mexico, molybdenum deposit: ECONOMIC GEOLOGY, v. 89, p. 1780–1802.

Concha, A., Oyarzun, R., Lunar, R., and Sierra, J., 1991, Over a century of bioleaching copper sulphides at Andacollo: Mining Magazine, 1991, p. 324–327.

Cuadra, W.A., and Dunkerley, P.M., 1991, A history of gold in Chile: Economic Geology, v. 86, p. 1155–1173.

Dong, G., and Morrison, G.W., 1995, Adularia in epithermal veins, Queensland: Morphology, structural state and origin: Mineralium Deposita, v. 30, p. 11–19.

Gustafson, L.B., and Hunt, J.P., 1975, The porphyry copper deposit at El Salvador: ECONOMIC GEOLOGY, v. 70, p. 859–912.

Haas, J.L., 1971, The effect of salinity on the maximum thermal gradient of a hydrothermal system at hydrostatic pressure: ECONOMIC GEOLOGY, v. 66, p. 940–946.

Hayba, D.O., Bethke, P.M., Heald, P., and Foley, N.K., 1985, Geologic, mineralogic, and geochemical characteristics of volcanic-hosted epithermal precious-metal deposits: Reviews in ECONOMIC GEOLOGY, v. 2, p. 129–168.

Hedenquist, J.W., 1990, The thermal and geochemical structure of the Broadlands-Ohaaki geothermal system, New Zealand: Geothermics, v. 19, p. 151–185.

Henley, R.W., 1985, The geothermal framework for epithermal deposits: Reviews in ECONOMIC GEOLOGY, v. 2, p. 1–24.

Irvine, R.J., and Smith, M.J., 1990, Geophysical exploration for epithermal gold deposits: Association of Exploration Geochemists Special Publication 16b, p. 375–412.

Kaiser, L., 1942, Alteracion hidrotermal de la Formación Porfirítica en Andacollo: Congreso Panamericano de Ingeniería de Minas y Geología, Santiago, 1942, Proceedings, v. 2, p. 467–478.

Levi, B., Nyström, J.O., Thiele, R., and Åberg, G., 1987, Geochemical polarities in Mesozoic-Tertiary volcanic rocks from the Andes in central Chile and tectonic implications: Journal of South American Geology, v. 1, p. 63–74.

Llaumet, C., 1975, Faja Pacífica de cobres porfídicos y desarrollos de alteración hidrotermal en Chile: Congreso Iberoamericano de Geología Económica, 2nd, Buenos Aires, 1975, v. 2, p. 331–348.

—— 1983, Geología, mineralización y evaluación de reservas del yacimiento aurífero de Andacollo: La Serena, Chile, Sociedad Minera Aurífera Geraldo, unpublished report, 81 p.

Lowell, J.D., and Guilbert, J.M., 1970, Lateral and vertical alteration-mineralization zoning in porphyry ore deposits: ECONOMIC GEOLOGY, v. 65, p. 373–408.

Müller, R., 1986, Geología y mineralización del distrito aurífero de Andacollo (30°14′30″S, 71°06′30″W) IV región, Chile: Universidad de La Serena (Chile), Departamento de Ingeniería de Minas, unpublished report, 61 p.

Müller, R., Helle, S., and Oyarzún, J., 1988, Rocas alcalinas versus metasomatismo alcalino en la zona aurífera de Churrumata, distrito de Andacollo, Chile: Congreso Geológico Chileno, 5th, Santiago, 1988, Proceedings, v. 3, p. G99-G112.

Nash, J.T., 1976, Fluid inclusion petrology-data from porphyry copper deposits and applications to exploration: U.S. Geological Survey Profesional Paper 907-D, 16 p.

Potter, R.W., Jr., Babcock, R.S., and Brown, D.L., 1977, A new method for determining the solubility of salts in aqueous solutions at elevated temperatures: U.S. Geological Survey Journal of Research, v. 5, p. 389–395.

Ramboz, C., Pichavant, M., and Weisbrod, A., 1982, Fluid inmiscibility in natural processes. Use and misuse of fluid inclusion data. II. Interpretation of fluid inclusion data in terms of inmiscibility: Chemical Geology, v. 37, p. 29–48.

Reyes, M., 1991, The Andacollo strata-bound gold deposit, Chile, and its position in a porphyry copper-gold system: ECONOMIC GEOLOGY, v. 86, p. 1301–1316.

Rivano, S., and Sepulveda, P., 1991, Hoja Illapel, Carta Geológica de Chile no. 69, scale 1: 250,000: SERNAGEOMIN (Servicio Nacional de Geología y Minería, Santiago de Chile), 132 p.

Roedder, E., 1971, Fluid inclusion studies on the porphyry-type ore deposits at Bingham, Utah, Butte, Montana and Climax, Colorado: ECONOMIC GEOLOGY, v. 66, p. 98–120.

—— 1984, Fluid inclusions: Reviews in Mineralogy, v. 12, 646 p.

Sillitoe, R.H., 1981, Regional aspects of the Andean porphyry copper belt in Chile and Argentina: Institution of Mining and Metallurgy Transactions,v. 90, sec. B., p. 15–36.

—— 1983, Styles of low-grade gold mineralization in volcano-plutonic arcs: Nevada Bureau of Mines and Geology Paper 36, p. 56–68.

—— 1989, Gold deposits in western Pacific island arcs: The magmatic connection: ECONOMIC GEOLOGY MONOGRAPH 6, p. 274–291.

—— 1991, Gold metallogeny of Chile—an introduction: ECONOMIC GEOLOGY, v. 86, p. 1187–1205.

Sutton, F.M., and McNabb, A., 1977, Boiling curves at Broadlands geothermal field, New Zealand: New Zealand Journal of Science, v. 20, p. 333–337.

Twiss, R.J., and Moores, E.M., 1992, Structural geology: New York, W.H. Freeman and Company, 532 p.

White, N.C., and Hedenquist, J.W., 1990, Epithermal environments and styles of mineralizations: Variations and their causes, and guidelines for exploration: Association of Exploration Geochemists Special Publication 16b, p. 445–474.

Zentilli, M., 1974, Geological evolution and metallogenic relationships in the Andes of northern Chile between 26° and 29° south: Unpublished Ph.D. thesis, Kingston, Ontario, Canada, Queen's University, 446 p.